International Journal of Electrical and Computer Engineering (IJECE)
Vol. 12, No. 6, December 2022, pp. 5872~5879
ISSN: 2088-8708, DOI: 10.11591/ijece.v12i6.pp5872-5879

Higher chromatic rendition with Cr^{3+}-doped yellow $Y_3Al_5O_{12}:Ce^{3+}$ for double-layer remote phosphor white-light-emitting diodes

Dieu An Nguyen Thi[1], Phuc Dang Huu[2], Thuy Hang Nguyen Thi[3]
[1]Faculty of Electrical Engineering Technology, Industrial University of Ho Chi Minh City, Ho Chi Minh City, Vietnam
[2]Institute of Applied Technology, Thu Dau Mot University, Binh Duong Province, Vietnam
[3]Faculty of General Science, University of Natural Resources and Environment of Ho Chi Minh City, Ho Chi Minh City, Vietnam

Article Info

Article history:

Received Aug 5, 2021
Revised Jun 14, 2022
Accepted Jul 7, 2022

Keywords:

Color uniformity
Luminous flux
Mie-scattering theory
$Y_3Al_5O_{12}:Ce^{3+},Cr^{3+}$

ABSTRACT

Remote phosphor designs of white-light-emitting diodes (WLEDs) have been recognized for their high thermal stability and excellent luminous efficiency but not for the chromatic rendering. The study presents an approach for the remote phosphor structure to overcome the low-color-rendering issue by enriching its red-light spectral intensity through co-doping Cr^{3+} and Ce^{3+} ions into the yellow $Y_3Al_5O_{12}$ (YAG) phosphor compound. This ion co-doping process probably enhances emission spectra in the far-red range because of the energy transfer of the integrated ions: Ce^{3+} Cr^{3+}. Additionally, the luminescence and color properties of the phosphor layer significantly depend on the doped concentration of the Cr^{3+} ion. Here, with 0.008% Cr^{3+} in the phosphor composite, either internal or external quantum performances of the dual-layer WLED light are enhanced, which achieved the number of 58.9% and 46.7%, respectively. The color rendering index (CRI) would also be higher if Cr^{3+} is added, about 77.9, compared to the CRI of 63.2 when using the original YAG:Ce^{3+} phosphor layer.

Corresponding Author:

Phuc Dang Huu
Institute of Applied Technology, Thu Dau Mot University
No 6, Tran Van on Street, Thu Dau Mot city, Binh Duong Province, Vietnam
Email: danghuuphuc@tdmu.edu.vn

1. INTRODUCTION

The white-light-emitting diodes (WLEDs) that use phosphors for the task of transmuting illumination generated by the blue light-emitting diode (LED) chip have been widely used in solid-state illuminating solutions. This can be credited to their outstanding features, which include long lifetime, short operation time, excellent luminesce, high robustness, cost and energy efficiencies, and eco-friendliness, over other lighting sources [1]–[3]. One of the most common phosphors utilized in WLED coating fabrication is the yellow phosphor of cerium yttrium aluminum garnet ($Y_3Al_5O_{12}:Ce^{3+}$ or YAG:Ce^{3+}) [4]. In spite of its popularity, the LED using YAG:Ce^{3+} coating layer has been struggling in yielding high chromatic rendering performances because of lacking red-spectral region, a crucial factor for a good-chromatic-rendition light source. This is therefore a barrier that restricts further developments of this phosphor-converted LED type in wide-range illuminating applications [5], [6]. Thus, the potential solution is to enrich the red spectral region in the emission spectrum of the white light. The ion Cr^{3+} was added to alternate the Ce^{3+} for this objective. The red emission peaks at the far range of phosphor YAG:Cr^{3+} were observed in 650-750 nm, in addition to the two main absorption peaks at the wavelengths of 430 nm and

600 nm. Nevertheless, the lighting excitation of this phosphor was inefficient as d-d transitions of Cr^{3+} ions were not allowed [7]. On the other hand, the original YAG:Ce^{3+} possesses great excitation performance that peaks under 458 nm wavelength thanks to the allowed d-f transitions [8], as well as one broad emission range from 450 to 700 nm that overlaps the absorption peaks of the Cr^{3+} ion. The power shift between Ce^{3+} and Cr^{3+} within the Cr^{3+}-doped YAG:Ce^{3+} was analyzed and resulted in a deep red emission centering at 690 nm, and low thermal quenching [9], as well as the dipole-quadrupole interaction [10].

This study uses the YAG:Ce^{3+},Cr^{3+} yellow-red phosphor to fabricate a double-layer remote configuration for the white LED models. It is believed that with the enriched far-red range in the emission spectrum, the color quality of the WLED will be enhanced considerably. The chromaticity of the WLED will be evaluated via three factors including the color variation, color rendering index (CRI), as well as color quality scale (CQS). The luminous intensity is also examined to check the performance of red-yellow YAG:Ce^{3+},Cr^{3+} phosphor. It is also noted that high color adequacy could be attained with minor degradation of the luminescence when applying Ce^{3+}-Cr^{3+} co-doped YAG phosphors.

2. RESEARCH METHOD

2.1. Preparation of yellow-red-emitting $Y_3Al_5O_{12}:Ce^{3+},Cr^{3+}$ phosphor

The preparation of the yellow-red $Y_3Al_5O_{12}:Ce^{3+},Cr^{3+}$ was carried out via solid-state reaction at high temperatures. The concentration of each doped ion is 2% wt. for Ce^{3+} and 0%-1.5% wt. for Cr^{3+}. The ingredients of this phosphor include Y_2O_3, Al_2O_3, CeO_2, Cr_2O_3 weighed in a stoichiometric amount. BaF_2 was added with the concentration of 5% wt. to be a flux, while oleic acid used at 1% wt. was utilized as a dispersant. All the ingredients were mixed by ball milling in ethanol in a 100-ml alumina ball mill nylon bottle, which lasted 6 hours. After that, the attained product was put on a glass culture surface, then let dry under a temperature of 80 °C in twelve hours. An agate mortal was employed to ground the mixture, which was placed within a crucible made of alumina afterwards. A 5-hour firing stage was carried out at 1,500 °C under the condition of 5%H_2/95%N_2. When the heating process finished, the product was cooled down and reground in an agate mortar [10]–[12].

A D8 Advance Bruker θ–2θ diffractometer X-ray powder diffraction (Cu Kα X-radiation, λ=1.54060 Å) were used to collect the XRD data of the prepared yellow-red $Y_3Al_5O_{12}:Ce^{3+},Cr^{3+}$ samples. Standard JCPDS files were applied to provide the phase identification, while the morphologies of the phosphor surfaces were specified by using JSM-670 scanning electron microscopy (JEOL, Japan). The photoluminescence and photoexcitation were collected at room temperature via a fluorescence spectrometer model F-7000 (Hitachi, Japan), with the setting of excitation of λ_{ex}=450 nm or via observation under λ_{em}=707 nm [13]–[15]. The quantum yield of the phosphor was measured by the F-7000 spectrometer coupled with an optical sphere. The F-4600 spectrometer using a 400 V photomultiplier tube and a Xenon light under 150 watts was employed for the measurements of photoluminescence depending on temperatures. Additionally, the fluorescence lifetime imaging was taken using an ISA FluorologTau-3 spectrophotometer with an excitation source being the Xenon light mentioned. The light characteristics in WLED models, including hue coordinates, color rendering, color temperature, along with luminous flux, were measured by a system integrating optical and electric assessment of Hangzhou Everfine Photo-E-Info [16], [17]. The blue chip was set to 60 milliamperes forward current during the measurement.

2.2. Phosphors' luminescent spectra

The YAG:Ce^{3+} without doping Cr^{3+} ions exhibited three peaks of excitation spectra: 230 nm, 340 nm, as well as 458 nm. The 230 nm excitation line was from the 4f ground state → 5d sub-band electron transition. The other excitation peaks were attributed to the shifts between ground status 4f and the power levels $5d_1$ (for 340 nm) and $5d_2$ (for 458 nm) [18], [19]. The broad-spectrum band of YAG:Ce^{3+} was also observed, a result possibly caused by the 5d → 4f shift in the ion of Ce^{3+}.

The YAG:Cr^{3+} (without ion Ce^{3+}) showed excitation peaks under 280 nm, 430 nm, as well as 592 nm, which was caused by the electrons' transitions between ground status $^4A_2$ and excited statuses of $^4T_1(^4P)$, $^4T_1(^4F)$ and $^4T_2(^4F)$, in turn [12]. In addition to that, the emission spectra of the red ion Cr^{3+} demonstrated several emissions peaks in the far-red region, including 677 nm, 688 nm, 707 nm, as well as 726 nm, resulting from the transition of ^2E → $^4A_2$. As can be seen, an overlap in the Cr^{3+} excitation band and the Ce^{3+} emission band was displayed, indicating that the energy transfer between Ce^{3+} and Cr^{3+} can be attributed to the non-radioactive power shift related to the resonance mechanism of the donor-acceptor pair.

In terms of the YAG:Ce^{3+},Cr^{3+}, the luminescence spectrum at 340 nm excitation wavelength includes both yellow and red emission ranges, owing to the presence of the yellow ion Ce^{3+} and red ion

Cr^{3+}. Moreover, when observing the emission spectra of the phosphor at 707 nm, the absorption peak wavelengths at 340 nm and 458 nm of Ce^{3+} are recorded. Thus, the energy transfer between the two ions considerably boosts the red spectral energy. Besides, at 0.8% doped Cr^{3+}, the flux intensity of the phosphor reaches the highest values. The efficiencies in internal and external quantum yields, and absorption properties, collected at this 0.8% concentration of Cr^{3+}, are 58.9%, 46.7%, and 79.4%, respectively.

To provide a more in-depth understanding of the energy transfer Ce^{3+}→Cr^{3+}, the mathematical module is demonstrated. According to Paulose's report [13], the energy transfer between two ions Ce^{3+} and Cr^{3+} can be described as [13], [20]–[23]:

$$\eta_{ET} = 1 - \frac{\tau_s}{\tau_{so}} \quad (1)$$

In which, η_{ET} indicates the efficiency in the transfer of energy, τ_s is the decay durations for the Ce^{3+} sensitizer when the Cr^{3+} trigger exists, while that in the absence of Cr^{3+} activator is the presented by τ_{so}. At different concentrations of Cr^{3+}, the energy transfer performances show significant changes. Specifically, the collected η_{ET} at 0%, 0.3 %, 0.8%, and 1.5% concentration of Cr^{3+} are 0%, 56.88%, 73.91%, 81.49%, and 87.42%, respectively.

The resonance mechanism in the energy transfer between the sensitizers and activators is usually performed through the exchange or multipolar interaction [24]. In terms of the exchange interaction, it is noted that an overlapping orbital of the donor-acceptor pair is essential. The shorter range separating the sensitizer and activator is required to remain below 3-4 Å [25]. With the energy transfer mechanism proposed by Dexter, the exchange interaction and the multipolar interaction can be described in (2) and (3), respectively.

$$ln\left(\frac{\eta_0}{\eta}\right) \propto C \quad (2)$$

$$\frac{\eta_0}{\eta} \propto C^{\alpha/3} \quad (3)$$

Here, η_0 and η show the performance of the Ce^{3+} luminescent quantum in the absence and presence of Cr^{3+}, in turn. C indicates the content for the Ce^{3+} and Cr^{3+} doped to the phosphor composite. In (3), α is set at 6, 8, and 10; representing dipole-dipole, dipole-quadrupole, and quadrupole-quadrupole interactions, respectively. $\frac{\eta_0}{\eta}$ value could be relatively equal to the ratio of luminous intensity $\frac{I_0}{I}$ whose computation can be described as (4), (5).

$$ln\left(\frac{I_0}{I}\right) \propto C \quad (4)$$

$$\frac{I_0}{I} \propto C^{\alpha/3} \quad (5)$$

The 3-D simulated design program of LightTools 9.0 accompanied with the Monte Carlo method is used to simulate WLED structure. Accordingly, the phosphor layers of the WLED model are simulated based on the flat layer of silicone. The design was initially defined and the focus lighting features of the WLED model were then chosen and added. Next, the concentration of $Y_3Al_5O_{12}$:Ce^{3+},Cr^{3+} phosphor was adjusted and the changes in WLED optical performances were then closely monitored and examined. The color temperatures of the LED models were set at 5000 K and 6500 K. The point of experimenting on two different color temperatures is to compare and evaluate the influences of the new phosphor $Y_3Al_5O_{12}$:Ce^{3+},Cr^{3+} on the WLED with dual-layer remote structure.

From the evaluated optical results, it is possible to figure out the effective approach to advance the quality of dual-layer WLED lights. The physical illustration of the WLED model is shown in Figure 1. The conformal phosphor coating method was applied here, indicating that the $Y_3Al_5O_{12}$:Ce^{3+},Cr^{3+} was not included. The specifications of the common LED model can be described as follows. A reflector was designed with bottom span measured at 8 mm, top length measured at 9.85 mm, and height measured at 2.07 mm. In the reflector's cavity, there were 9 LED chips connected in parallel and coated with a 0.08-mm thick phosphor layer. The radiant flux of each chip reach 1.16 W with peak wavelength reaching 453 nm.

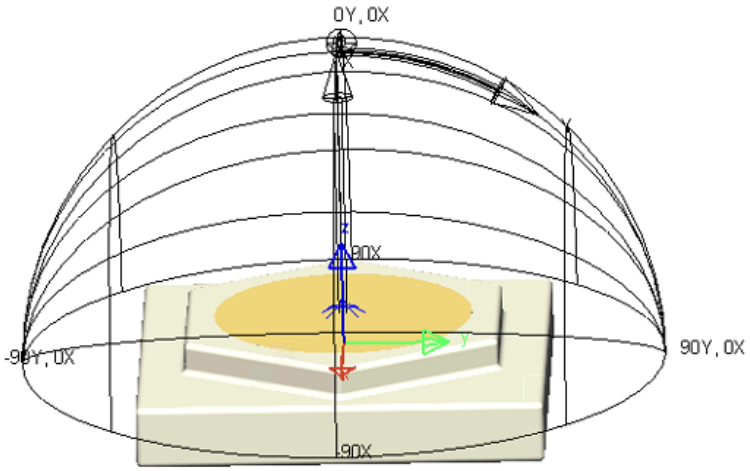

Figure 1. Photograph of a WLED sample

3. RESULTS AND DISCUSSION

The change in the yellow-red phosphor $Y_3Al_5O_{12}:Ce^{3+},Cr^{3+}$ concentration leads to the fluctuation of the original yellow YAG:Ce^{3+} phosphor concentration. As the stability of the WLED correlated color temperatures (CCTs) at 5,000 K and 6,500 K is an important factor for a high-quality WLED, the YAG:Ce^{3+} content suffers from a penalty along with the rising concentration of $Y_3Al_5O_{12}:Ce^{3+},Cr^{3+}$. This is clearly demonstrated in Figures 2(a) and 2(b). In addition to that, the reduction of the yellow phosphor YAG:Ce^{3+} has incredible impacts on the performance of light absorption and scattering features, leading to the change in both chromaticity and luminescence of the WLED lights. In other words, the percentage of $Y_3Al_5O_{12}:Ce^{3+},Cr^{3+}$ phosphor in the dual-layer phosphor configuration of WLED would be among the most vital facets determining the hue output and luminous efficiency in a WLED model. As can be clearly seen, the lowest level of YAG:Ce^{3+} can be observed when there is 20% wt. $Y_3Al_5O_{12}:Ce^{3+},Cr^{3+}$ in the structure, regardless of the CCTs.

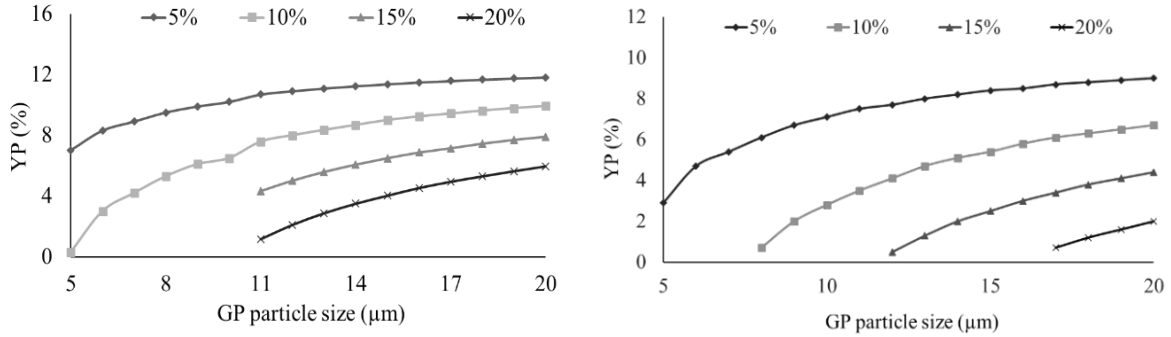

(a) (b)

Figure 2. Retaining median CCT through altering phosphor content (a) 5,000 K and (b) 6,500 K

The emission spectra of the double-layer remote phosphor structure with $Y_3Al_5O_{12}:Ce^{3+},Cr^{3+}$ presence, monitored at CCTs of 5,000 K and 6,500 K, are displayed in Figures 3(a) and 3(b), respectively. The addition of the $Y_3Al_5O_{12}:Ce^{3+},Cr^{3+}$ layer probably enhances the strength of the spectral regions of blue, yellow-green and red lights (420–480 nm, 500–640 nm as well as 680–720 nm, in turn). In particular, the higher intensities of 420–480 nm and 500–640 nm indicate that the luminous flux is boosted, while the stronger emission in 680–720 nm demonstrates better color rendering ability of the light source. Additionally, this $Y_3Al_5O_{12}:Ce^{3+},Cr^{3+}$ helps to enhance the scattering of the emitted blue lights, implying the improved scattering feature of the remote phosphor layer configuration, which contributes greatly to heightening the chromatic uniformity of the WLED light. Besides, the double-layer remote phosphor structure usually faces

difficulties in managing good color uniformity at high color temperature (over 5,000 K), but using $Y_3Al_5O_{12}:Ce^{3+},Cr^{3+}$ as the second phosphor film can give a solution to this. The scattering events in the simulated WLED models at both 5,000 K and 6,500 K present considerable enhancements. In other words, $Y_3Al_5O_{12}:Ce^{3+},Cr^{3+}$ could effectively manage to accomplish good color rendering value at not only low but also high CCTs. This is probably a crucial factor for the production of modern WLED lighting devices.

The efficiency of using $Y_3Al_5O_{12}:Ce^{3+},Cr^{3+}$ to enhance the luminous intensity of the WLED is specifically demonstrated in Figure 4. In both graphs, as the concentration of $Y_3Al_5O_{12}:Ce^{3+},Cr^{3+}$ increases (5%-20% wt.), the luminous flux is also lifted, regardless of the color temperature, see Figure 4(a). Moreover, the increase in $Y_3Al_5O_{12}:Ce^{3+},Cr^{3+}$ content leads to better color homogeneity since the scattering is enhanced, which critically minimizes the angular color variation, as shown in Figure 4(b). The higher the percentage of the yellow-red emitting phosphor, the smaller the variation of color presents, at both pre-set CCTs, which is exhibited via Figure 5. To demonstrate this influence, the absorption feature of $Y_3Al_5O_{12}:Ce^{3+},Cr^{3+}$ phosphor is taken into consideration, see Figure 5(a). As the original green-yellow emitting YAG:Ce^{3+} is enriched with ion Cr^{3+} for the red-light enhancement in the total light emission, it has the LED-chip blue lights absorbed and subsequently converted into red lights, thus, leading to a better color balance, as shown in Figure 5(b). Though the Cr^{3+}-doped YAG:Ce^{3+} also takes in the yellow light from the original YAG:Ce^{3+} phosphor film, the amount of blue light absorbed is much larger. Thus, there are more color components of red generated, leading to the higher color homogeneity metric of the white light. The WLED light that possesses a high chromatic uniformity index probably has a higher price in the illuminating market; and $Y_3Al_5O_{12}:Ce^{3+},Cr^{3+}$ is one of the cost-efficiency phosphor materials, thus it can help to save the production cost when being used in the large-scale manufacture.

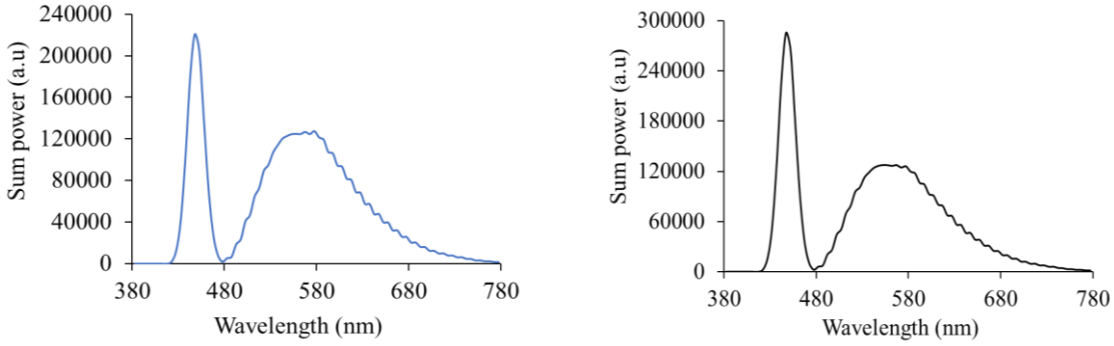

(a) (b)

Figure 3. Correlation between discharge spectra in WLED device and Y3Al5O12:Ce3+,Cr3+ addition: (a) 5,000 K and (b) 6,500 K

Besides the hue consistency, the CRI and CQS would also be important facets to evaluate the chromatic faithfulness of a light source. Thus, it is essential to examine both CRI and CQS of the double-layer WLED models using $Y_3Al_5O_{12}:Ce^{3+},Cr^{3+}$ phosphor layer to demonstrate further on the yellow-red phosphor's effectiveness in WLED-chromaticity improvement. The color rendering metrics of the WLED at two CCTs of 5,000 K and 6,500 K are presented in Figures 6(a) and 6(b), while their CQS parameters are exhibited via Figures 7(a) and 7(b). Though the CRI is benefited by the red spectral energy, it shows a downward trend as the concentration of $Y_3Al_5O_{12}:Ce^{3+},Cr^{3+}$ becomes higher, which can be attributed to the imbalance in color distribution since the generated red light components are more than the others. On the other hand, the CQS exhibit relatively stability with $Y_3Al_5O_{12}:Ce^{3+},Cr^{3+}$ concentration around 10% wt. When comparing the CQS and the CRI, the CQS is more effective than the CRI as it includes CRI in its evaluating aspects. Additionally, the CQS examines the color preference of the human visuality and the color coordinates. Thus, the WLED with high CQS might process higher brightness and color truthfulness than the other ones. Similar to the CRI, the CQS decreases when the concentration of $Y_3Al_5O_{12}:Ce^{3+},Cr^{3+}$ is over 10% wt. Hence, choosing the concentration of the $Y_3Al_5O_{12}:Ce^{3+},Cr^{3+}$ phosphor plays a crucial role in manufacturing high-quality WLED lamps. It is also noted that, if the WLED light requires excellent color quality parameters, the luminous intensity might be slightly decreased, yet this small reduction is probably acceptable since the light loss caused by the back-scattering phenomenon is reduced, while the light transmission and conversion are both improved with the $Y_3Al_5O_{12}:Ce^{3+},Cr^{3+}$ supplement in the package.

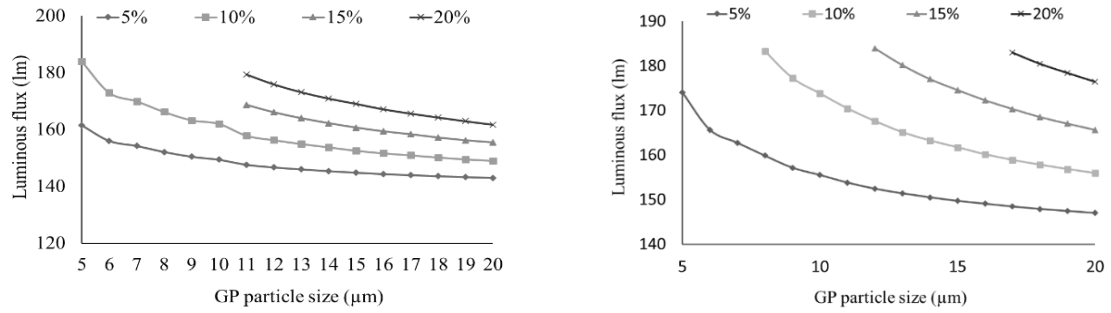

Figure 4. Correlation between lumen in WLED device and $Y_3Al_5O_{12}:Ce^{3+},Cr^{3+}$ concentrations (a) 5,000 K and (b) 6,500 K

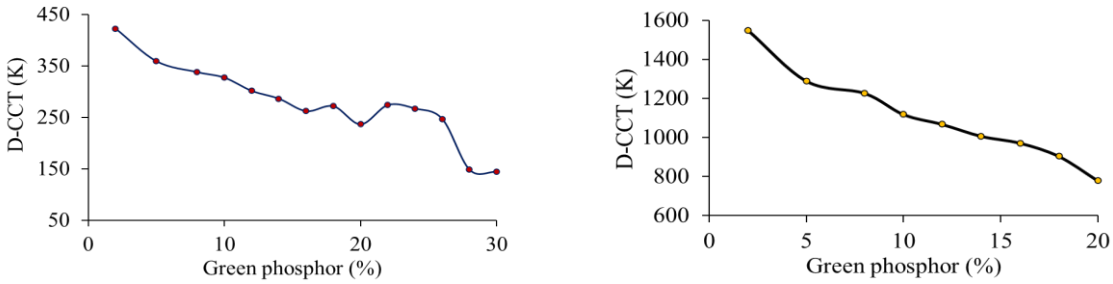

Figure 5. Correlation between lumen in WLED device and $Y_3Al_5O_{12}:Ce^{3+},Cr^{3+}$ concentrations (a) 5,000 K and (b) 6,500 K

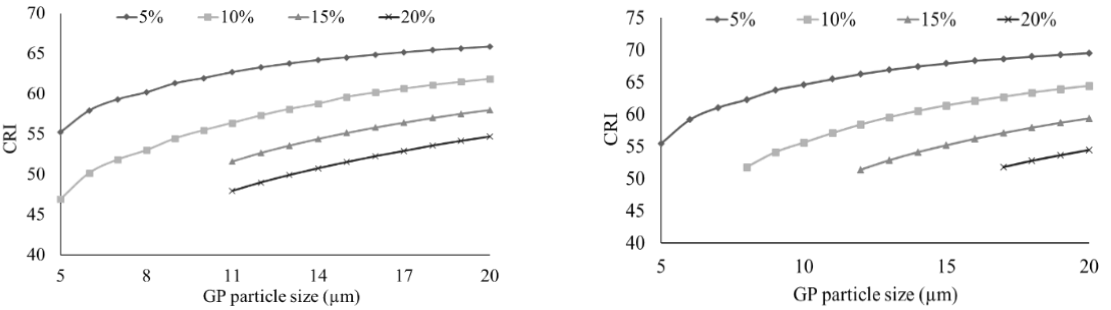

Figure 6. Correlation between CRI in WLED device and Y3Al5O12:Ce3+,Cr3+ concentrations (a) 5,000 K and (b) 6,500K

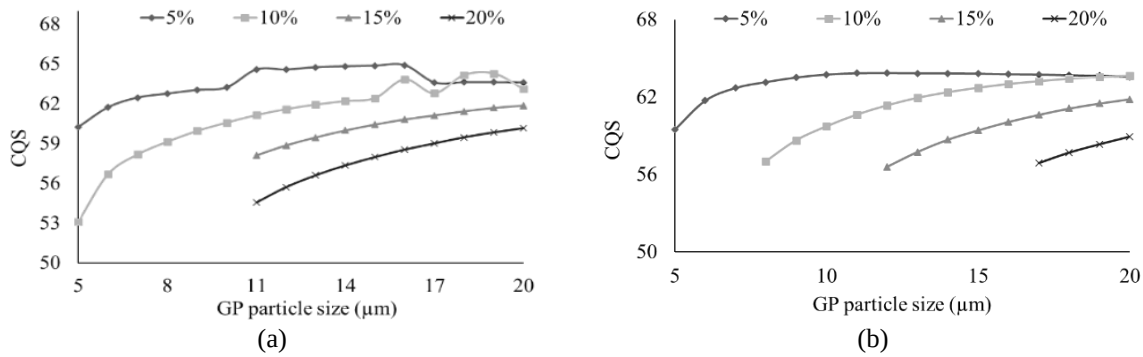

Figure 7. Correlation between CQS in WLED device and $Y_3Al_5O_{12}:Ce^{3+},Cr^{3+}$ concentrations (a) 5,000 K and (b) 6,500K

4. CONCLUSION

The yellow-red YAG:Ce^{3+},Cr^{3+} phosphor's benefits in enhancing the color performance of double-layer WLEDs are reported in this research. The recommended doped concentration of Cr^{3+} ion is 0.8% wt. while the Ce^{3+} concentration is constant at 0.2% wt., since the red emission intensity of the phosphor at this Cr^{3+} concentration is the highest. With the enriched red component by Cr^{3+}, the color properties of the white LED are enhanced significantly. The color rendering index can be achieved at nearly 80, which is much higher than that of the YAG:Ce^{3+} (at about 63.2). Besides, the study pointed out that the YAG:Ce^{3+},Cr^{3+} content in the double-layer remote phosphor package has great effects on the lumen as well as the hue features. The rise of YAG:Ce^{3+},Cr^{3+} concentration (5%-20% wt.) leads to the improvement of the luminescence and degradation of color deviation. On the other hand, the chromatic parameters, including the CRI and CQS, are stable at relative high levels with the concentration of YAG:Ce^{3+},Cr^{3+} below 10% wt. If the yellow-red phosphor is added (more than 10% wt.), CRI and CQS gradually decrease due to the excessive amount of red components, leading to the imbalance in color distribution. Thus, if the CQS and CRI are the main goals, it is acceptable to have a small reduction in the luminescence intensity.

ACKNOWLEDGEMENTS

This research is supported by Industrial University of Ho Chi Minh City (IUH) under grant number 121/HD-DHCN.

REFERENCES

[1] J.-H. Kim, B.-Y. Kim, and H. Yang, "Synthesis of Mn-doped CuGaS_2 quantum dots and their application as single downconverters for high-color rendering solid-state lighting devices," *Optical Materials Express*, vol. 8, no. 2, Jan. 2018, doi: 10.1364/ome.8.000221.

[2] Y.-C. Jen *et al.*, "Design of an energy-efficient marine signal light based on white LEDs," *OSA Continuum*, vol. 2, no. 8, Aug. 2019, doi: 10.1364/osac.2.002460.

[3] Y. Fang *et al.*, "Giant enhancement of white light emission from $Ca_9Ln(PO_4)_7$:Eu^{2+},Mn^{2+} (Ln = La, Lu, Gd) phosphors achieved by remote aluminum reduction," *Optical Materials Express*, vol. 10, no. 5, May 2020, doi: 10.1364/ome.390069.

[4] Q. Guo *et al.*, "Characterization of YAG:Ce phosphor dosimeter by the co-precipitation method for radiotherapy," *Applied Optics*, vol. 60, no. 11, Apr. 2021, doi: 10.1364/ao.419800.

[5] H. Yuce, T. Guner, S. Balci, and M. M. Demir, "Phosphor-based white LED by various glassy particles: control over luminous efficiency," *Optics Letters*, vol. 44, no. 3, Jan. 2019, doi: 10.1364/ol.44.000479.

[6] Z. Zhang, W. Li, N. Ma, and X. Huang, "High-brightness red-emitting double-perovskite phosphor Sr_2LaTaO_6:Eu^{3+} with high color purity and thermal stability [Invited]," *Chinese Optics Letters*, vol. 19, no. 3, 2021, doi: 10.3788/col202119.030003.

[7] D. T. Tuyet *et al.*, "Deep red fluoride dots-in-nanoparticles for high color quality micro white light-emitting diodes," *Optics Express*, vol. 28, no. 18, Aug. 2020, doi: 10.1364/oe.400848.

[8] S. Matsumoto and A. Ito, "Chemical vapor deposition route to transparent thick films of Eu^{3+}-doped HfO_2 and Lu_2O_3 for luminescent phosphors," *Optical Materials Express*, vol. 10, no. 4, Mar. 2020, doi: 10.1364/ome.386425.

[9] C. Tian *et al.*, "Mn^{4+} activated Al_2O_3 red-emitting ceramic phosphor with excellent thermal conductivity," *Optics Express*, vol. 27, no. 22, Oct. 2019, doi: 10.1364/oe.27.032666.

[10] R. Wan *et al.*, "Simultaneously improve the luminous efficiency and color-rendering index of GaN-based white-light-emitting diodes using metal localized surface plasmon resonance," *Optics Letters*, vol. 44, no. 17, Aug. 2019, doi: 10.1364/ol.44.004155.

[11] S. K. Abeysekera, V. Kalavally, M. Ooi, and Y. C. Kuang, "Impact of circadian tuning on the illuminance and color uniformity of a multichannel luminaire with spatially optimized LED placement," *Optics Express*, vol. 28, no. 1, Dec. 2020, doi: 10.1364/oe.381115.

[12] C. Wu *et al.*, "Phosphor-converted laser-diode-based white lighting module with high luminous flux and color rendering index," *Optics Express*, vol. 28, no. 13, Jun. 2020, doi: 10.1364/oe.393310.

[13] W. J. Kim *et al.*, "Improved angular color uniformity and hydrothermal reliability of phosphor-converted white light-emitting diodes by using phosphor sedimentation," *Optics Express*, vol. 26, no. 22, Oct. 2018, doi: 10.1364/oe.26.028634.

[14] Y. Li, X. Zhang, H. Yang, X. Yi, J. Wang, and J. Li, "Effects of remote sediment phosphor plates on high power laser-based white light sources," *Optics Express*, vol. 29, no. 15, Jul. 2021, doi: 10.1364/oe.433581.

[15] A. A. Pan'kov, "Informative light pulses of indicating polymer fiber-optic piezoelectroluminescent coatings upon indentation of rigid globular particles," *Journal of Optical Technology*, vol. 88, no. 8, Aug. 2021, doi: 10.1364/JOT.88.000477.

[16] M. Nourry-Martin, P. Pichon, F. Druon, S. Darbon, F. Balembois, and P. Georges, "Light recycling in LED-pumped Ce:YAG luminescent concentrators," *Optics Express*, vol. 29, no. 16, Jul. 2021, doi: 10.1364/oe.433063.

[17] J.-S. Li, Y. Tang, Z.-T. Li, L.-S. Rao, X.-R. Ding, and B.-H. Yu, "High efficiency solid–liquid hybrid-state quantum dot light-emitting diodes," *Photonics Research*, vol. 6, no. 12, Nov. 2018, doi: 10.1364/prj.6.001107.

[18] T. Y. Orudzhev, S. G. Abdullaeva, and R. B. Dzhabbarov, "Increasing the extraction efficiency of a light-emitting diode using a pyramid-like phosphor layer," *Journal of Optical Technology*, vol. 86, no. 10, pp. 671–676, Oct. 2019, doi: 10.1364/JOT.86.000671.

[19] H. Liu, Y. Shi, and T. Wang, "Design of a six-gas NDIR gas sensor using an integrated optical gas chamber," *Optics Express*, vol. 28, no. 8, pp. 11451–11462, Apr. 2020, doi: 10.1364/OE.388713.

[20] P. D. Huu, P. T. That, T. T. Trang, P. X. Le, and N. D. Q. Anh, "Benefits of using TiO2 quantum dots in producing low-cost and high-quality white light-emitting diodes," *TELKOMNIKA (Telecommunication Computing Electronics and Control)*, vol. 20, no. 3, pp. 656–662, Jun. 2022, doi: 10.12928/telkomnika.v20i3.15347.

[21] Y. Ma *et al.*, "Broadband emission $Gd_3Sc_2Al_3O_{12}$:Ce^{3+} transparent ceramics with a high color rendering index for high-power white LEDs/LDs," *Optics Express*, vol. 29, no. 6, Mar. 2021, doi: 10.1364/OE.417464.

[22] J. Hao, H.-L. Ke, L. Jing, Q. Sun, and R.-T. Sun, "Prediction of lifetime by lumen degradation and color shift for LED lamps, in a non-accelerated reliability test over 20,000 h," *Applied Optics*, vol. 58, no. 7, Mar. 2019, doi: 10.1364/ao.58.001855.
[23] Y.-P. Chang *et al.*, "New scheme of LiDAR-embedded smart laser headlight for autonomous vehicles," *Optics Express*, vol. 27, no. 20, Sep. 2019, doi: 10.1364/oe.27.0a1481.
[24] T. P. White, E. Deleporte, and T.-C. Sum, "Feature issue introduction: halide perovskites for optoelectronics," *Optics Express*, vol. 26, no. 2, Jan. 2018, doi: 10.1364/oe.26.00a153.
[25] X. Ding *et al.*, "Improving the optical performance of multi-chip LEDs by using patterned phosphor configurations," *Optics Express*, vol. 26, no. 6, Mar. 2018, doi: 10.1364/oe.26.00a283.

BIOGRAPHIES OF AUTHORS

Dieu An Nguyen Thi received a master of Electrical Engineering, HCMC University of Technology and Education, Vietnam. Currently, she is a lecturer at the Faculty of Electrical Engineering Technology, Industrial University of Ho Chi Minh City, Vietnam. Her research interests are Theoretical Physics and Mathematical Physics. She can be contacted at email: nguyenthidieuan@iuh.edu.vn.

Phuc Dang Huu received a Physics Ph.D. degree from the University of Science, Ho Chi Minh City, in 2018. Currently, He is Research Institute of Applied Technology, Thu Dau Mot University, Binh Duong Province, Vietnam. His research interests include simulation LEDs material, renewable energy. He can be contacted at email: danghuuphuc@tdmu.edu.vn.

Thuy Hang Nguyen Thi received a Bachelor of Chemistry from Ho Chi Minh City Pedagogical University, Vietnam, Master in Organic Chemistry, Ho Chi Minh City University of Natural Sciences, Vietnam. Currently, she is a lecturer at the Faculty of General Science, University of Natural Resources and Environment of Ho Chi Minh City, Vietnam. Her research interests are Theoretical Physics and Mathematical Physics. She can be contacted at email: ntthuyhang@hcmunre.edu.vn.